INTERACTION NOTES

Note 258

September 1975

MEASURED CURRENTS AND CHARGES ON THIN CROSSED ANTENNAS IN A PLANE-WAVE FIELD

R. W. Burton
U.S. Naval Postgraduate School

and

R. W. P. King
Harvard University

ABSTRACT

Measured distribution of current and charge per unit length on electrically long and thin crossed antennas over a ground plane are displayed for five sets of lengths that locate the junction at minima and maxima of charge and include resonant and antiresonant combinations of lengths. The currents are induced by a normally incident plane electromagnetic wave with its electric vector parallel to one of the mutually perpendicular antennas. Attention is given to the behavior of currents and charges near the junction where Kirchhoff's current law and equality of charges per unit length are observed. For purposes of physical understanding a zero-order explanation of the distributions of charge per unit length and current is given in terms of resonant and forced components.

This research was supported in part by the Joint Services Electronics Program under Contract N00014-67-A-0298-0005 with Harvard University.

1. INTRODUCTION

The tangential magnetic field and the normal electric field on the surfaces of crossed metal structures like aircraft are of interest in determining the shielding properties of the metal skin when this is imperfectly conducting or has apertures. In order to understand the response to a pulse a knowledge of the induced distributions of surface current and charge over a wide range of frequencies is required. Since the determination of such distributions on structures that are electrically thick is difficult, attention is advantageously directed first to crossed electrically thin conductors in order to gain physical insight into the nature of the phenomena. Of particular interest is the behavior of the current and charge per unit length at and near the junction of crossed wires. A number of different and in some cases mutually exclusive assumptions have been made in the literature [1]-[5]. In order to clarify and resolve these it is desirable to provide an experimental study of the currents and charges induced on crossed electrically thin wires for configurations that include wires with a wide range of lengths and different locations of the junction in the standing-wave patterns. Meaningful physical interpretations are also sought.

2. REVIEW OF CURRENTS AND CHARGES ON AN ISOLATED PARASITIC CYLINDER

A review has already been made of the distributions of current and charge per unit length induced in an isolated electrically thin conductor in an incident plane-wave field [6] as a means of standardizing an experimental procedure in terms of available theoretical analyses [7]-[9] and in order to obtain an understanding of the properties of forced and resonant distributions of current and the associated charges. These results provide an important background for the study of crossed wires. They can be summarized

briefly in terms of the theoretical curves in Figs. 1 and 2. These illustrate the experimentally confirmed [6] theoretical distributions of current and charge per unit length along electrically thin conducting cylinders that are antiresonant (Fig. 1) and resonant (Fig. 2) as computed from the long antenna theory of Wu [8]. Each cylinder is in a normally incident electric field parallel to its axis. The origin of coordinates is at the center of a dipole or at the base of a monopole erected on a large, highly conducting ground plane. The currents vanish at $z = \pm h$, the charges per unit length at $z = 0$.

For qualitative purposes the distributions of charge per unit length, $q(z)$, in both Figs. 1 and 2 are quite well approximated in zero-order by $q(z) \sim \sin kz$ except at and very near $kz = n\pi$, $n = 0, 1, 2, \ldots$. The electrical distance between successive maxima (minima) in the standing-wave pattern is π, the actual distance is a half wavelength. Note, however, that for the antiresonant length represented in Fig. 1, $q(h) = 0$; whereas for the resonant length in Fig. 2, $q(h) = q_{max}$.

The forced current in antiresonant antennas with dipole half-lengths (or monopole lengths) given by $kh = n\pi$, n integral, are approximated in zero-order by $I(z) \sim \cos kz - \cos kh$. In a higher-order representation zeros are replaced by very small minima. In Fig. 1, $kh = 3\pi$ so that $I(z) \sim \cos kz + 1$. It is seen in Fig. 1 that the electrical distance between successive maxima (minima) in the standing-wave pattern of the forced current is 2π, the actual distance a full wavelength. It follows that minima of charge per unit length occur alternately at both maxima and minima of the forced current. Also, maxima of charge can occur at points intermediate to the maxima and minima of the forced current. The phase angle θ_I of the forced current is relatively constant; in particular, it never changes by π as does the phase angle θ_q of

the charge per unit length.

The current in Fig. 2 is that induced in a resonant length of wire. However, it is not purely resonant since it necessarily also includes a forced component. This is superimposed on the resonant current to make the maxima alternately larger and smaller. The phase varies much more than that of the pure forced current in Fig. 1, but the presence of the forced component limits the cyclical variation to less than π.

The change from antiresonant to resonant currents is most easily understood from a study of the real and imaginary parts (referred to the incident electric field) as the length of the antenna is increased. This is shown in a succession of diagrams in Fig. 3. Starting at the top, the purely forced current along a dipole with electrical half-length $kh = 2\pi$ is shown. The imaginary part is essentially a shifted cosine of the form $I_I(z) \sim \frac{1}{2}(1 - \cos kz)$ except near $kz = 0$ where it has a minimum instead of a zero. The real part is sensibly constant except in the quarter wavelength near $z = h$ where it approaches zero. The second set of graphs is for $kh = 5\pi/2$, a resonant length. Note that both $I_I(z)$ and $I_R(z)$ are roughly of the form $A_J(1 \pm \cos kz) + B_J \cos kz$, $J = I$ or R, where A_J is the amplitude of the forced part, B_J that of the resonant part. Note that $A_R << B_R$ since $I_R(z)$ is almost purely resonant, $A_I >> B_I$ since $I_I(z)$ is primarily a forced component. At $kh = 3\pi$ in the next diagram, the purely forced distribution has returned, but now there is a maximum instead of a minimum of $I_I(z)$ at $z = 0$ so that $I_I(z) \sim \frac{1}{2}(1 + \cos kz)$. The change from $kh = 3\pi$ to $kh = 7\pi/2$ is shown in three steps to bring out the gradual change in amplitude of $I_R(z)$ over the entire range and the complete reversal in direction of $I_I(z)$ between $kh = 10.696$ and $kh = 10.995 = 7\pi/2$. Note that throughout the range of kh from 2π to $7\pi/2$, both $I_R(z)$ and $I_I(z)$ are quite well approximated by the simple form

$I_J(z) = A_J(1 \pm \cos kz) + B_J \cos kz$ where A_J and B_J are constants.

3. APPLICATION TO CROSSED WIRES

Let a horizontal conductor (length $\ell = \ell_1 + \ell_2$) be connected to the vertical conductor (length $h = h_1 + h_2$) as shown in Fig. 4a to produce four mutually perpendicular, confluent members with lengths h_1, h_2, ℓ_1 and ℓ_2 and a common junction at $x = 0$, $z = h_1$. Since the cross is standing on a conducting plane, it is equivalent to the upper half of the structure shown in Fig. 4b in which the lower half may be regarded as the image of the upper half. Note that since two junctions and coupling between two horizontal members are involved, the cross with image is analytically considerably more complicated than the isolated cross for which a complete analytical solution is available [10]. However, in order to measure distributions of current and charge on the four conductors near their junction, the arrangement in Fig. 4a is preferred since access to the interior of the tubular conductors in order to move probes without wires in the field is available from below the ground plane. It is anticipated that in due course the analysis of the single cross [10] will be extended to the cross with image so that a direct comparison between theory and the present experiment will be made possible.

The current and charge distributions shown in Figs. 1 and 2 are those excited on the vertical member in Fig. 4a with the cross absent by a normally incident plane wave with the electric vector parallel to the z axis. When the horizontal member of the cross is connected, there is no component of the incident field along its extension. Furthermore, there is no inductive coupling between the mutually perpendicular conductors. It follows that currents and charges induced in the horizontal member (and its image) are by capacitive coupling to the periodically varying charges distributed along the ver-

tical conductor. It follows directly that the degree of coupling and the magnitudes and distributions of the charges and currents induced in the horizontal wire must depend critically on the locations of the junction point in the standing-wave pattern of the charges along the vertical conductor. In particular, as seen from Figs. 1 and 2, the junction can be located at $kz = \pi$, a deep minimum of charge per unit length and an extreme value of the current. However, $kz = \pi$ is at a minimum of current in Fig. 1, a maximum in Fig. 2. Alternatively, the cross can be located at $kz = 3\pi/2$ which is a point of maximum charge in both Figs. 1 and 2, but quite different currents. In Fig. 1 the current is at an intermediate point between maximum and minimum; in Fig. 2 it is quite near a minimum. In the absence of inductive coupling, it is anticipated that the location of the junction in the standing-wave pattern of the charge per unit length will play the dominant role.

4. MEASURED CURRENTS AND CHARGES PER UNIT LENGTH

In an earlier study [6] the experimental procedures for measuring distributions of current and charge per unit length were described and their accuracy verified by detailed comparisons of measured and theoretical distributions for a range of lengths of the vertical element shown in Fig. 4a but without the cross. The conductor was located in a normally incident linearly polarized electromagnetic wave with E^{inc} parallel to the axis. A simple extension of their procedures was carried out with the crossed member present and with probes traveling continuously along the forward surfaces of both the horizontal and the vertical members for distances of approximately a quarter wavelength from the junction at the lowest frequency. As before, two frequencies f_A and f_B were used such that with a fixed length h_1 the cross was located at $kh_1 = \pi$ with f_A and at $kh_1 = 3\pi/2$ with f_B. With f_A and with the

junction at $kh_1 = \pi$ (minimum charge at junction in vertical standing-wave pattern) the lengths of the horizontal members were chosen to be $k\ell_1 = k\ell_2 = \pi/2$ (minimum charge at junction in the horizontal standing-wave pattern). The vertical section above the junction was successively assigned the values $kh_2 = \pi/2$ and $kh_2 = 2\pi$ in order to locate first a minimum, then a maximum of current in the vertical standing-wave pattern at the junction. The two sets of measured charges per unit length and currents in amplitude and phase are shown in Figs. 5 and 6 both on the four members of the cross and, for ready comparison, on the vertical section alone. At f_B and with the junction at $kh_1 = 3\pi/2$ (maximum charge at the junction in the vertical standing-wave pattern) the lengths of the horizontal members were chosen to be $k\ell_1 = k\ell_2 = \pi$ (maximum charge at the junction in the horizontal standing-wave pattern). The vertical section above the junction was again successively assigned two values, viz., $kh_2 = \pi$ and $kh_2 = 2\pi$ in order to locate different relative currents at the junction. The two sets of measured amplitudes and phases of charges per unit length and currents are shown in Figs. 7 and 8 on the cross and on the vertical section alone. Finally, currents and charges per unit length were studied on a conductor with length $kh = 7\pi/4$ with the cross connected to make $kh_1 = 3\pi/4$, $kh_2 = \pi$. In this case, as shown theoretically in Fig. 9, the currents and charges at $kz = 3\pi/4$ on the vertical section alone are both large but not near their maxima. When an asymmetrical horizontal section is connected across such a vertical section at $kz = kh_1 = 3\pi/4$ with $kh_2 = \pi$, $k\ell_1 = \pi/2$, $k\ell_2 = \pi$, the measured charges per unit length and the currents are those shown in Fig. 10.

5. INTERPRETATION AND DISCUSSION OF MEASURED CURRENTS AND CHARGES

In order to understand the differences in the mutual interactions of charges on crosses with the junction at minima and maxima of charge per unit

length in the vertical and horizontal standing-wave patterns, it is instructive to consider the schematic diagrams in Figs. 11a,b. Fig. 11a shows the zero-order distribution of charge along the vertical conductor when the cross is located at the zero in the standing-wave pattern. Note that owing to symmetry, the charges in the two adjacent quarter wavelengths of the standing-wave distribution near the junction contribute mutually cancelling forces on charges at all points along the horizontal conductor. It follows that all non-cancelling forces must be due to quite distant charges. Moreover, as indicated in Fig. 11a, they have only very small components acting along the horizontal conductor to maintain equal and opposite currents in the two members when these have the same length. In contrast, Fig. 11b shows a cross located at a maximum of charge in the vertical standing-wave pattern. In this case the large concentrations of charges in the quarter wavelengths adjacent to the junction exert essentially uncancelled forces on charges in the adjacent portions of the horizontal wire in directions parallel to its axis. These act to induce currents.

The graphs in Fig. 5 show that the presence of the horizontal conductor when connected at a point of near-zero charge has very little effect on the currents and charges in the vertical cylinder. In the section h_1 between the ground plane and the junction only small changes in amplitude and phase are observed. Beyond the junction the current is decreased by the sum of the two small currents that are excited on the horizontal element. Kirchhoff's current law is obeyed and the charges per unit length in all four conductors are equal and very small at the junction. Note that the entire circuit is resonant in the sense that the combinations $h_1 + h_2$, $h_1 + \ell_1$, $h_1 + \ell_2$, $h_2 + \ell_1$, $h_2 + \ell_2$, and $\ell_1 + \ell_2$ are individually resonant circuits with maximum currents and minimum charges at the junction, maximum charges at the free ends. This

is illustrated in zero-order in Fig. 12a for the charges and in Fig. 12b for the currents.

The configuration in Fig. 6 differs from that in Fig. 5 only in that the lengths $h_1 + h_2$, $h_2 + \ell_1$ and $h_2 + \ell_2$ are antiresonant while $h_1 + \ell_1$, $h_1 + \ell_2$ and $\ell_1 + \ell_2$ are still resonant. This requires the part of the current associated with the circuit $h_1 + h_2$ to have a minimum instead of a maximum at the junction and to be distributed as a forced current. On the other hand, the parts of the current associated with $h_1 + \ell_1$ and $h_2 + \ell_2$ are resonant with maxima at the junction. This is illustrated in zero-order in Fig. 13a for the charges, in Fig. 13b for the currents. The effect of the horizontal conductor on the currents and charges in the vertical cylinder is greater than in Fig. 5 even though the junction is still a point of minimum charge per unit length for all conductors. This is a consequence of the existence of a current minimum at the junction for some circuits, a current maximum for others. The current in the length h_1 is increased substantially near the junction when the resonant circuits provided by the horizontal member are added. Again Kirchhoff's current law is obeyed and the charges per unit length in all four conductors are equal and very small at the junction.

The graphs in Figs. 7 and 8 show the currents and charges in crossed conductors that have resonant lengths in all of the six possible combinations: $h_1 + h_2$, $h_1 + \ell_1$, $h_1 + \ell_2$, $h_2 + \ell_1$, $h_2 + \ell_2$, $\ell_1 + \ell_2$. For each of these the junction is a point of maximum charge per unit length. As a consequence, all four conductors are very closely coupled capacitively near the junction. The currents and charges per unit length in the vertical conductor are markedly changed when the horizontal member is connected. Not only are the amplitudes greatly reduced on the vertical conductor but the shape of the current distribution curve changes completely. Superficially this may be

surprising since the horizontal conductors add only resonant circuits with a maximum of charge per unit length at the junction. The change in the current distribution is a consequence of the fact that forced currents can be induced only in the vertical parts of the several resonant circuits with associated distributions of charge per unit length that have zero values at the junction. It is seen from Fig. 14a in a qualitative zero-order manner that the inclusion of a forced component of charge per unit length on the length h_2 yields the correct form for the total charge in Fig. 8. The associated forced currents in the lengths h_1 and h_2 are shown in Fig. 14b. It is seen that with these the general shapes of the current amplitude curves in Fig. 8 are reproduced quite well. Figure 8 also shows that Kirchhoff's current law is obeyed and that the charges per unit length on all four conductors are the same at the junction.

A comparison of the measured currents and charges on the asymmetric cross shown in Fig. 10 with the currents and charges in Fig. 9 in the vertical member before the cross is attached reveals that the addition of the horizontal member has a very large effect on currents and charges especially in the length h_1. It is seen in Fig. 10 that the crossed antenna has large currents and charges per unit length on h_2, moderately large ones on h_1 and ℓ_1, very small ones on ℓ_2. How can these be explained? First it is to be noted that no combination of lengths of the four confluent conductors constitutes a resonant circuit. However, the forced current in the vertical length $h_2 = \lambda/2$ has a maximum at the junction as does the resonant current in the horizontal length $\ell_1 = \lambda/4$. A suitable combination of forced and resonant charges per unit length and associated currents as shown in a qualitative zero-order manner in Fig. 15 does provide total charges and currents very similar to the measured ones in Fig. 10. The currents shown in Fig. 10 satisfy Kirchhoff's

current law at the junction; the charges per unit length are equal on all four conductors at the junction.

6. CONCLUSIONS

Measurements of currents and charges per unit length along five different crossed antennas are shown graphically. These include junctions at points of minimum and maximum charge per unit length on symmetrical crosses and a junction at an intermediate point with an asymmetric cross. The disturbing effect of the cross arm and the currents and charges induced in it are extremely small when the junction is at a charge minimum, very large when it is at a charge maximum. The junction conditions are

$$\sum_{i=1}^{4} I_{i\,in} = 0 \tag{1}$$

$$q_1 = q_2 = q_3 = q_4 \tag{2}$$

where $I_{i\,in}$ is the current toward the junction in conductor i and q_i is the charge per unit length on conductor i at the junction. These conclusions apply specifically to circular conductors with radii $a_i \ll 1$, $i = 1, 2, 3, 4$, that satisfy the inequality $(ka_i)^2 \ll 1$ where k is the wave number of electromagnetic waves in air. In this case the chargeable surfaces of the junction are negligible and can be included approximately in the four conductors.

REFERENCES

[1] C. D. Taylor, "Electromagnetic scattering from arbitrary configurations of wires," IEEE Trans. Antennas Propagat., vol. AP-17, pp. 662-663, Sept. 1969.

[2] C. D. Taylor, S.-M. Lin and H. V. McAdams, "Scattering from crossed wires," IEEE Trans. Antennas Propagat., vol. AP-18, pp. 133-136, Jan. 1970.

[3] C. M. Butler, "Currents induced on a pair of skew-crossed wires," IEEE Trans. Antennas Propagat., vol. AP-20, pp. 731-736, Nov. 1972.

[4] H. H. Chao and B. J. Strait, "Radiation and scattering by a configuration of bent wires with junctions," IEEE Trans. Antennas Propagat., vol. AP-19, pp. 701-702, Sept. 1971.

[5] J. L. Lin, W. L. Curtis and M. C. Vincent, "Radar cross section of a rectangular conducting plate by wire-mesh modeling," IEEE Trans. Antennas Propagat., vol. AP-22, pp. 718-719, Sept. 1974.

[6] R. W. Burton and R. W. P. King, "Induced currents and charges on thin cylinders in a time-varying electromagnetic field," Interaction Note 257, August 1975.

[7] R. W. P. King, "Current distribution in an arbitrarily oriented receiving and scattering antenna," IEEE Trans. Antennas Propagat., vol. AP-20, pp. 152-159, March 1972.

[8] C.-L. Chen, "On the scattering of electromagnetic waves from a long wire," Radio Science, vol. 3, pp. 585-598, June 1968.

[9] C.-L. Chen and T. T. Wu, pp. 446-454 in Antenna Theory, Part I, R. E. Collin and F. J. Zucker, eds., McGraw-Hill, New York, 1969.

[10] R. W. P. King and T. T. Wu, "Analysis of crossed wires in a plane-wave field," Interaction Note 216, July 1974.

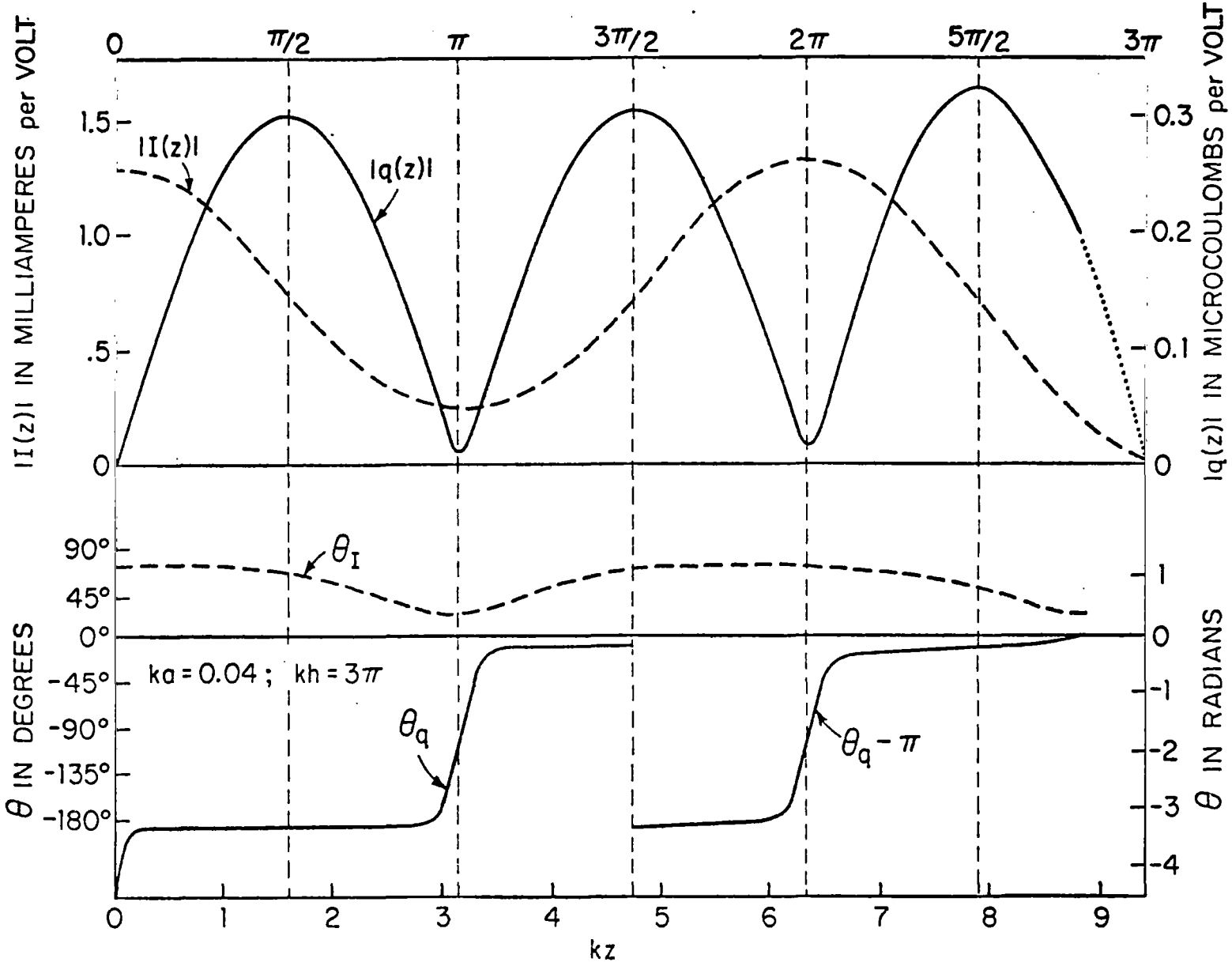

FIG. 1 THEORETICAL DISTRIBUTIONS OF CURRENT AND CHARGE IN PARASITIC ANTENNA IN NORMALLY INCIDENT FIELD, $h = 1.5\lambda$

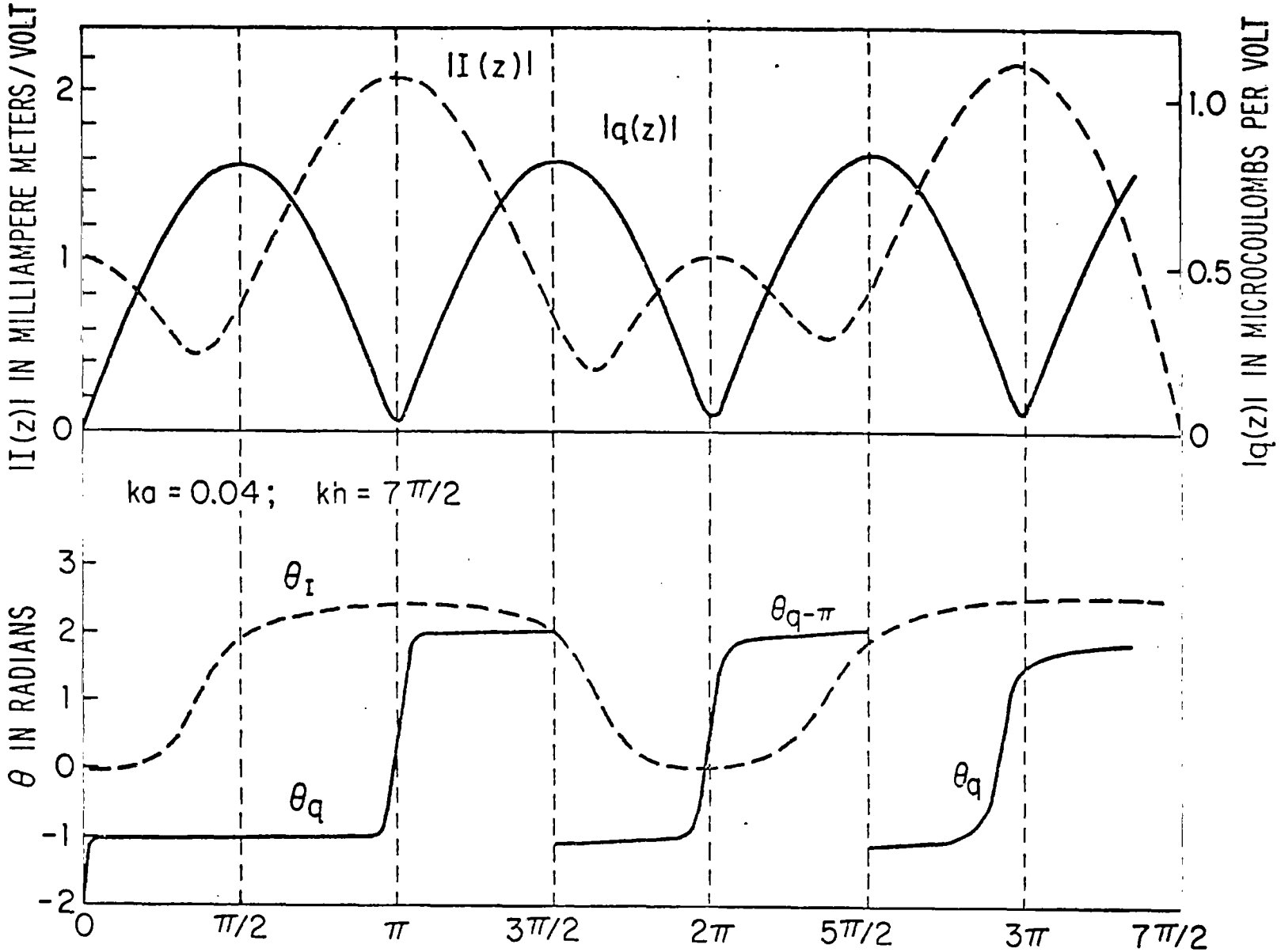

FIG. 2 THEORETICAL DISTRIBUTIONS OF CURRENT AND CHARGE PER UNIT LENGTH IN PARASITIC MONOPOLE IN NORMALLY INCIDENT FIELD ; $h = 7\lambda/4$

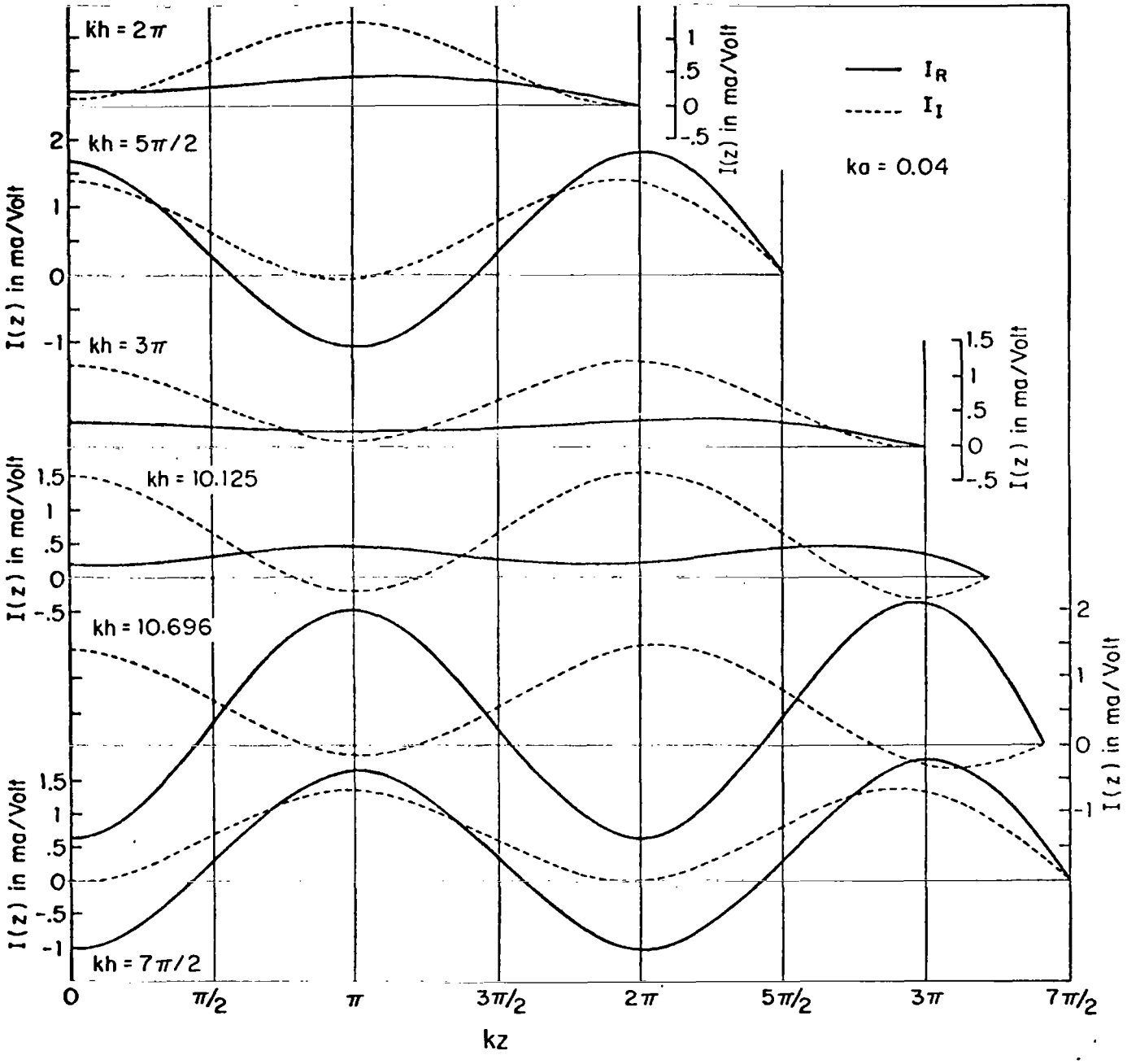

FIG. 3 REAL AND IMAGINARY CURRENTS ON PARASITIC ANTENNA IN NORMALLY INCIDENT FIELD

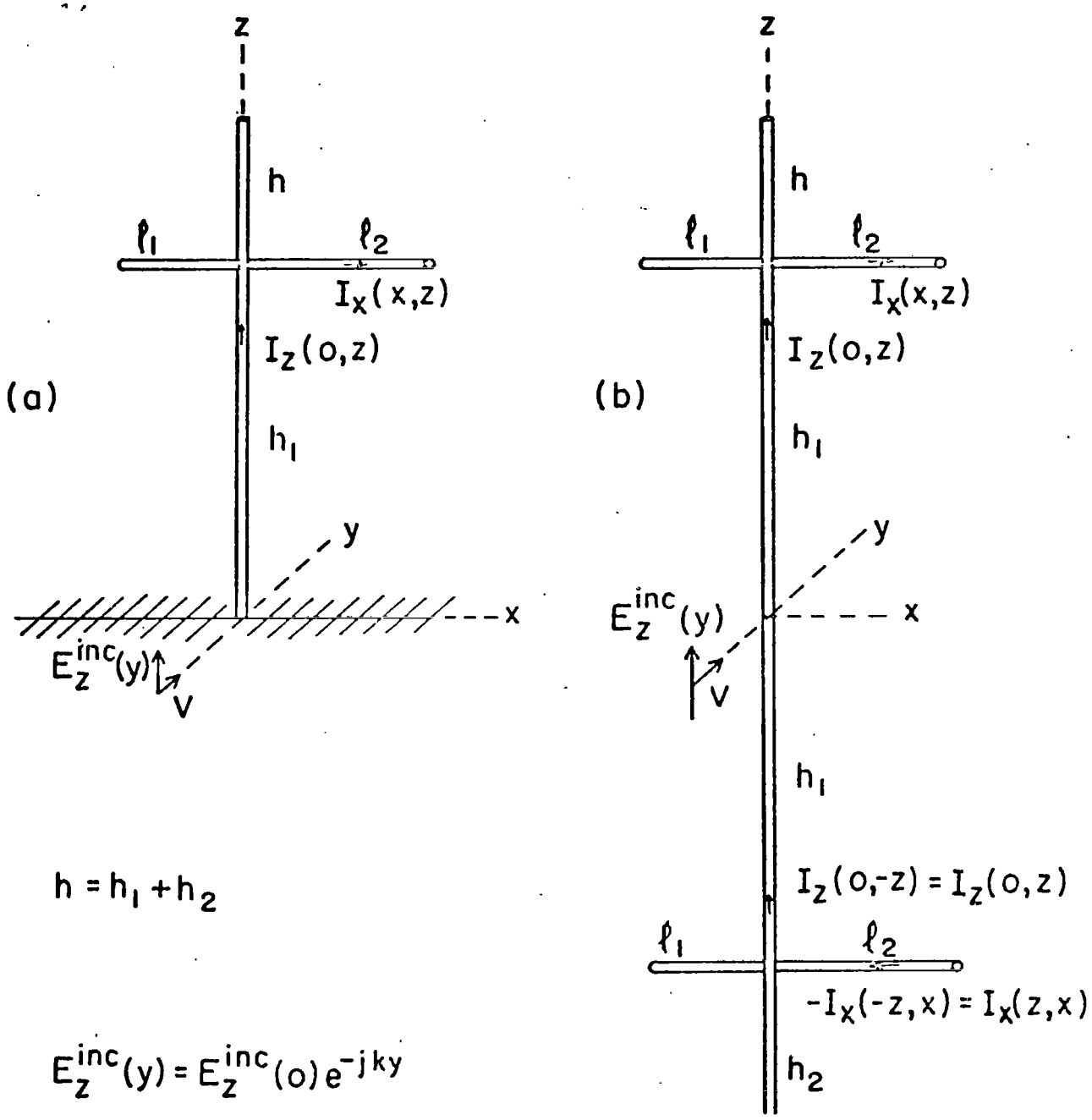

FIG. 4 (a) CROSSED ANTENNAS ON GROUND PLANE IN NORMALLY INCIDENT FIELD, (b) EQUIVALENT ISOLATED STRUCTURE, i,e., WITH IMAGE.

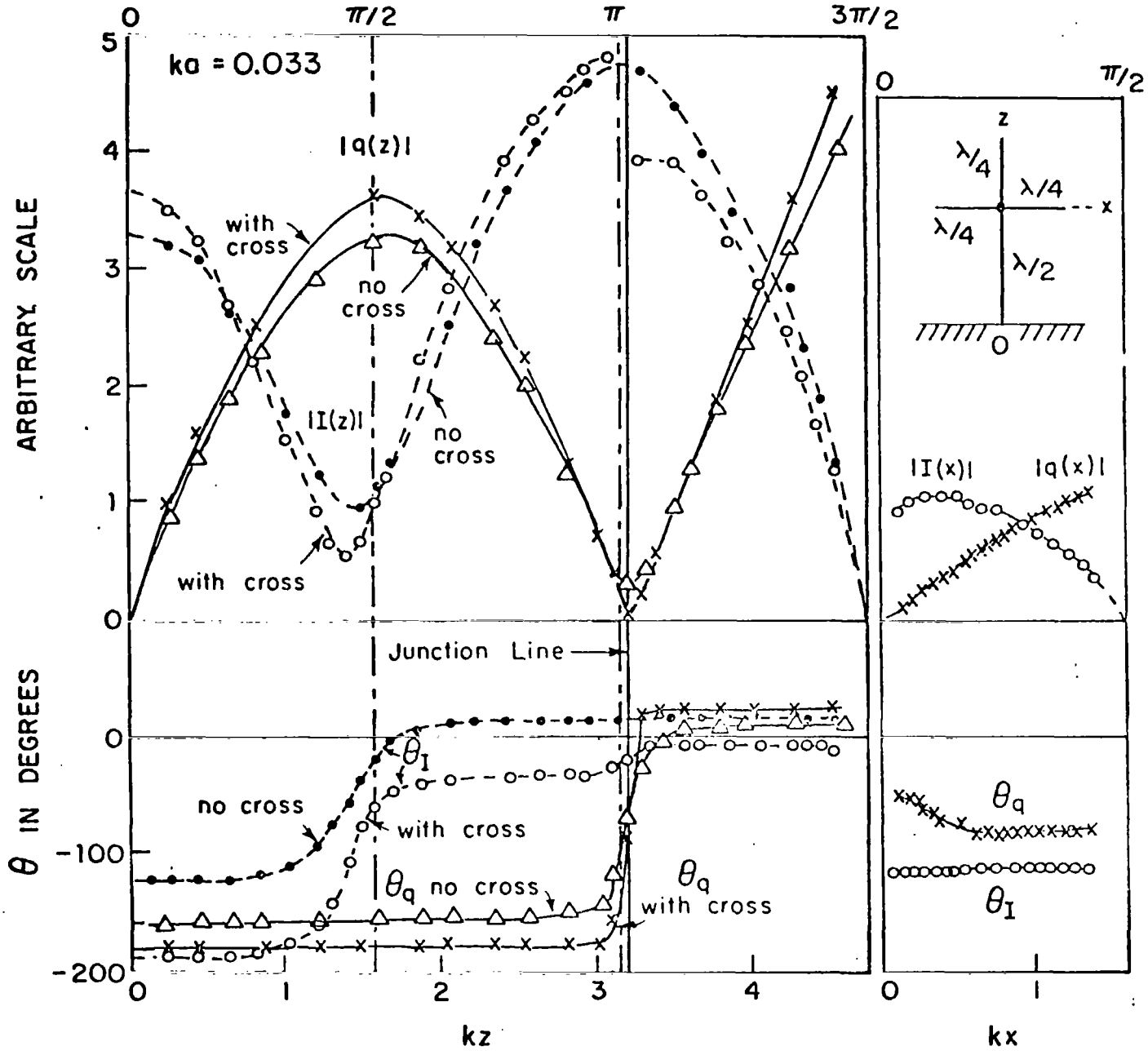

FIG. 5 MEASURED CURRENTS AND CHARGES PER UNIT LENGTH ON MONOPOLE AND CROSSED MONOPOLE IN INCIDENT FIELD. JUNCTION AT MAXIMUM CURRENT, MINIMUM CHARGE.

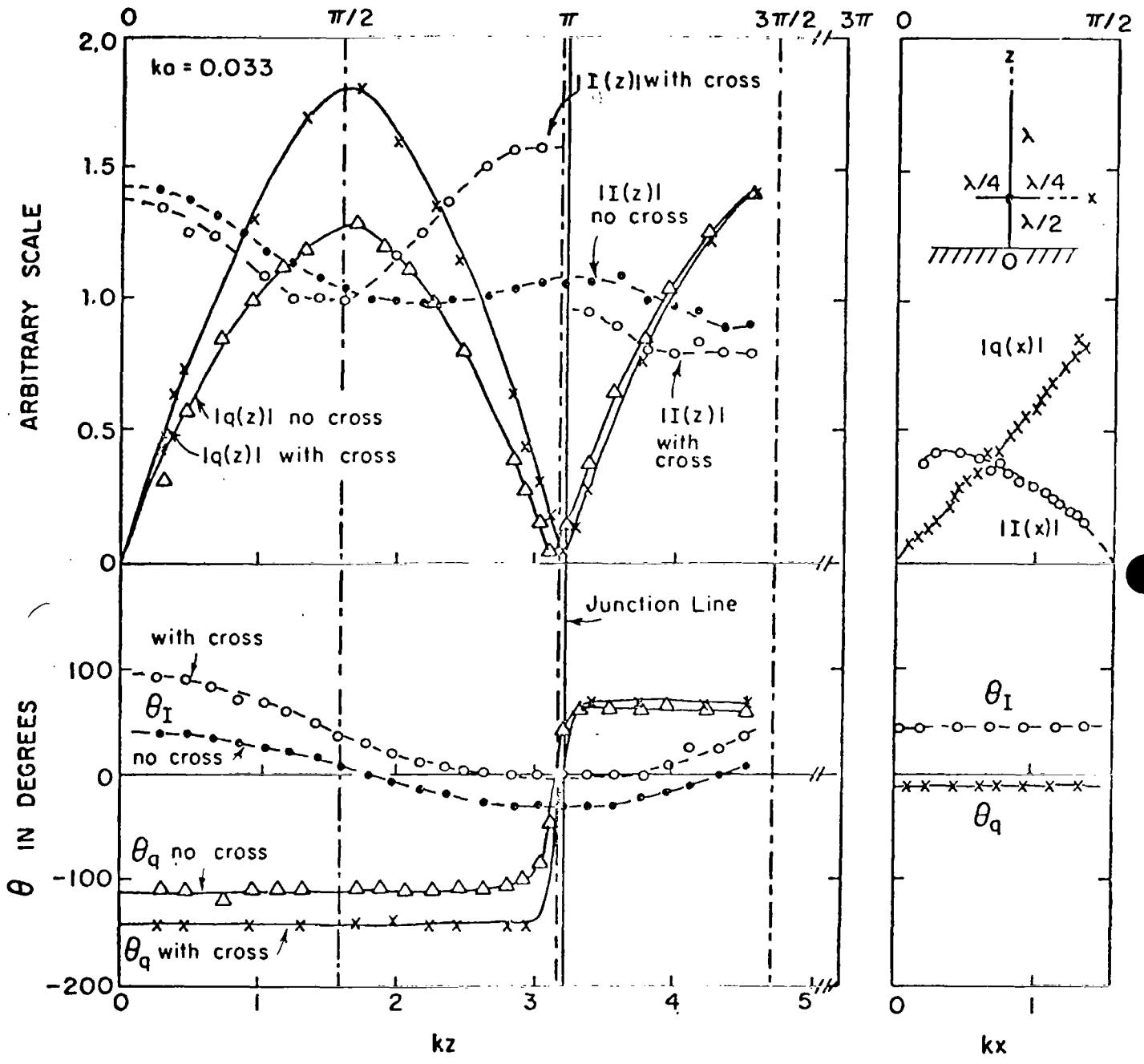

FIG. 6 MEASURED CURRENT AND CHARGE DISTRIBUTIONS ON ANTENNA WITH AND WITHOUT CROSS. JUNCTION AT MINIMUM OF CHARGE, MINOR MAXIMUM OF CURRENT

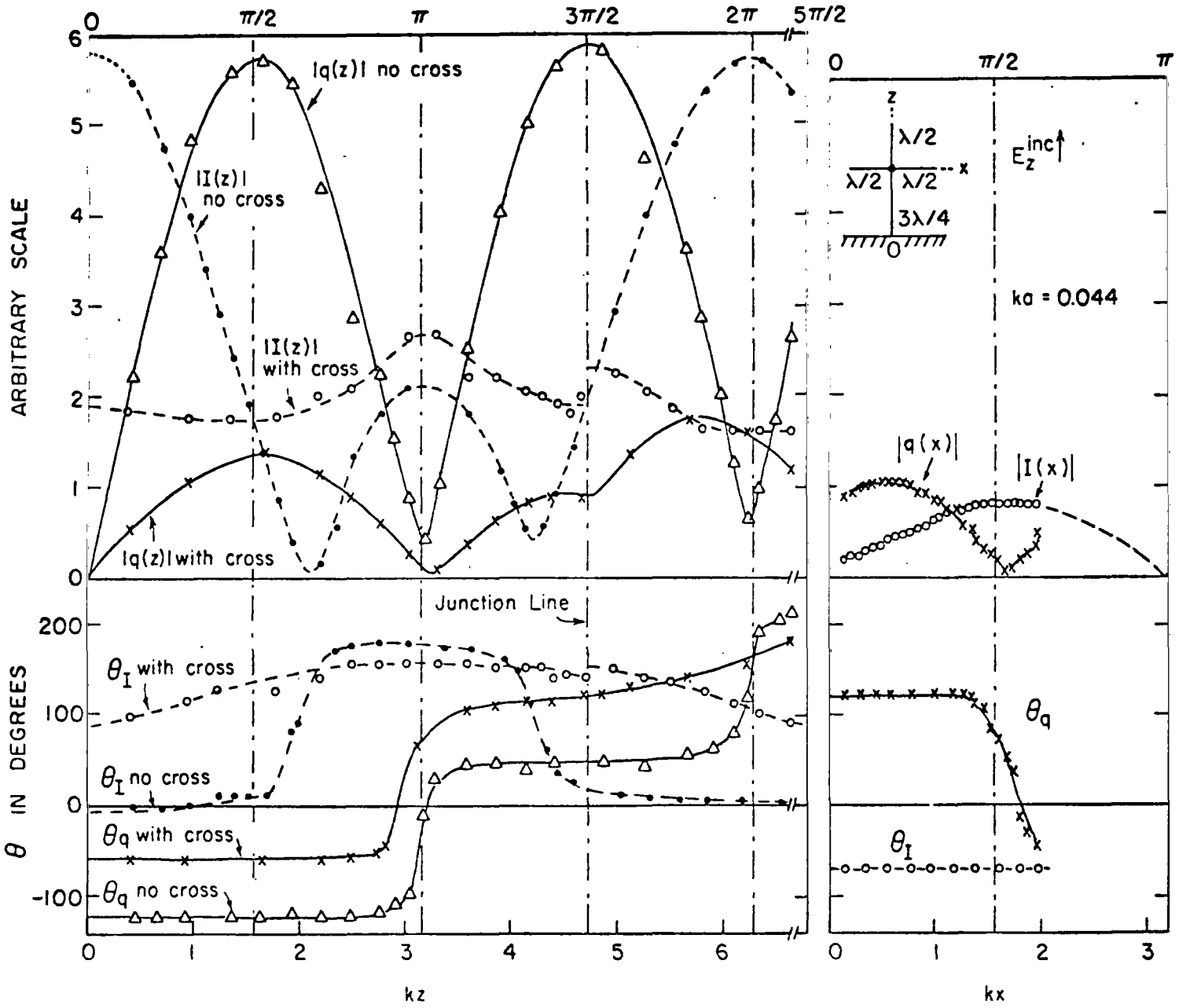

FIG. 7 MEASURED CURRENT AND CHARGE DISTRIBUTIONS ON ANTENNA WITH AND WITHOUT CROSS. JUNCTION AT MAXIMUM OF CHARGE

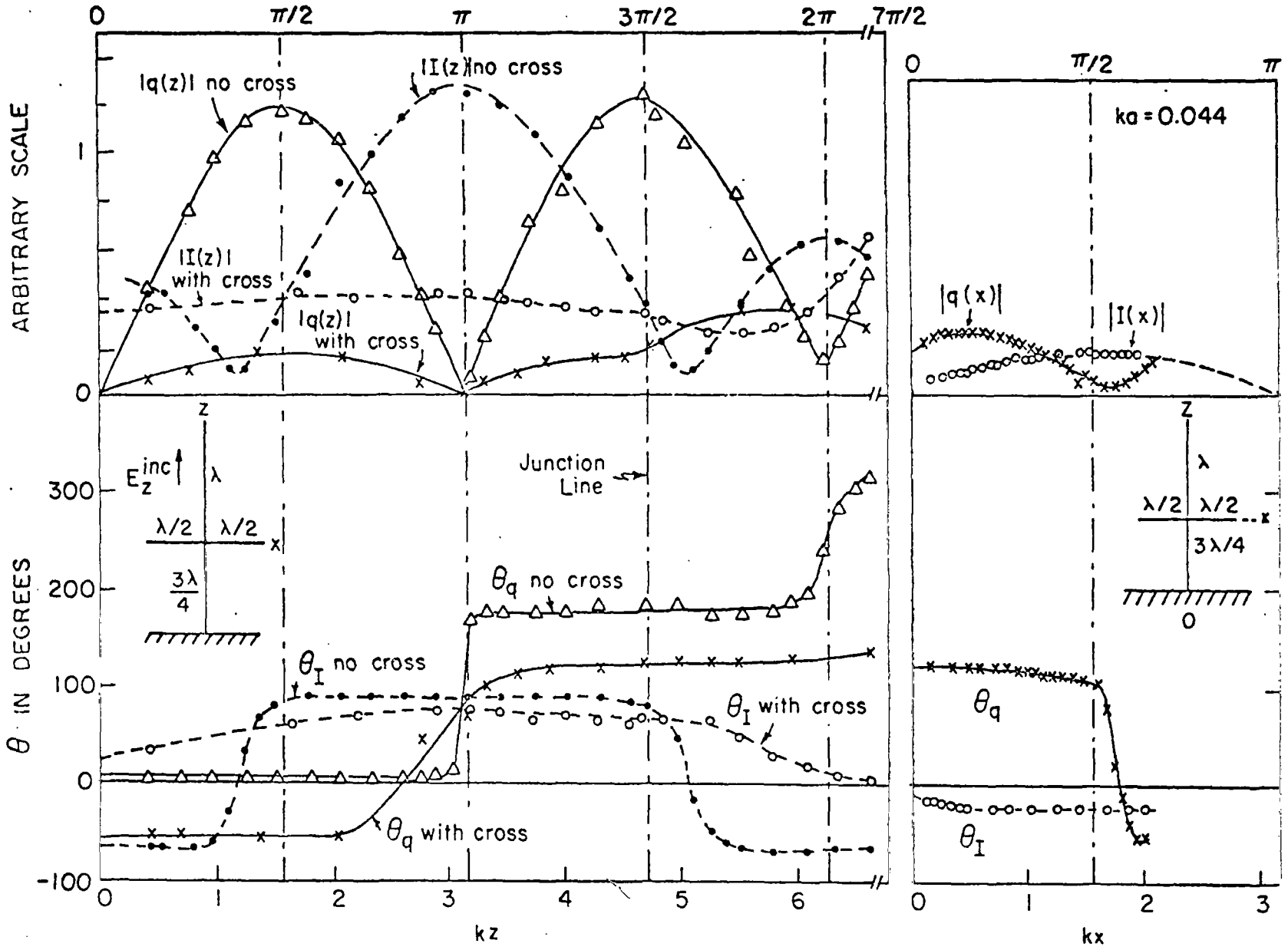

FIG. 8 MEASURED CURRENTS AND CHARGES PER UNIT LENGTH ON MONOPOLE AND CROSSED MONOPOLE IN INCIDENT FIELD. JUNCTION AT MINIMUM CURRENT, MAXIMUM CHARGE.

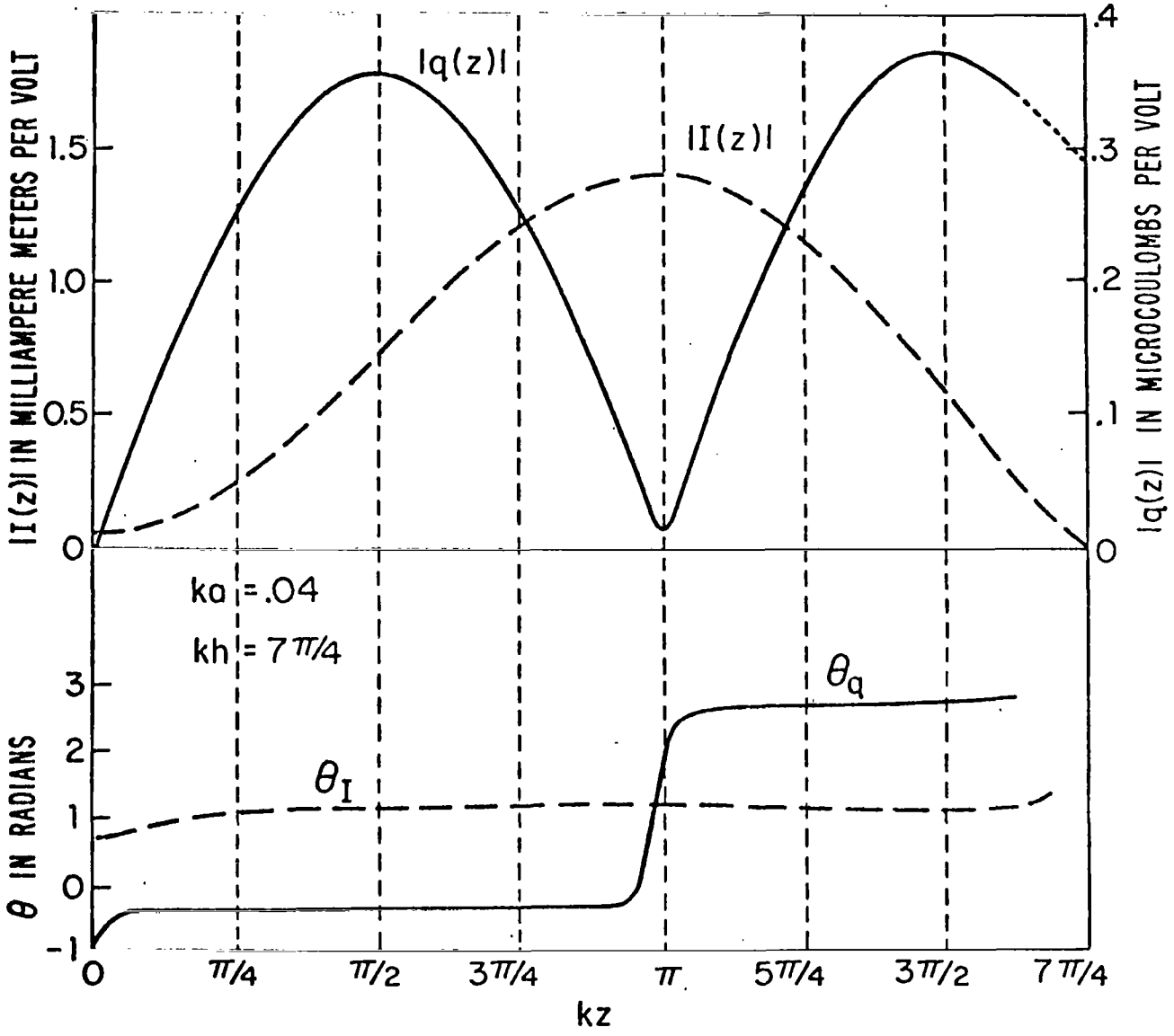

FIG. 9 THEORETICAL DISTRIBUTIONS OF CURRENT AND CHARGE PER UNIT LENGTH IN MONOPOLE IN NORMALLY INCIDENT FIELD ; $h = 7\lambda/8$

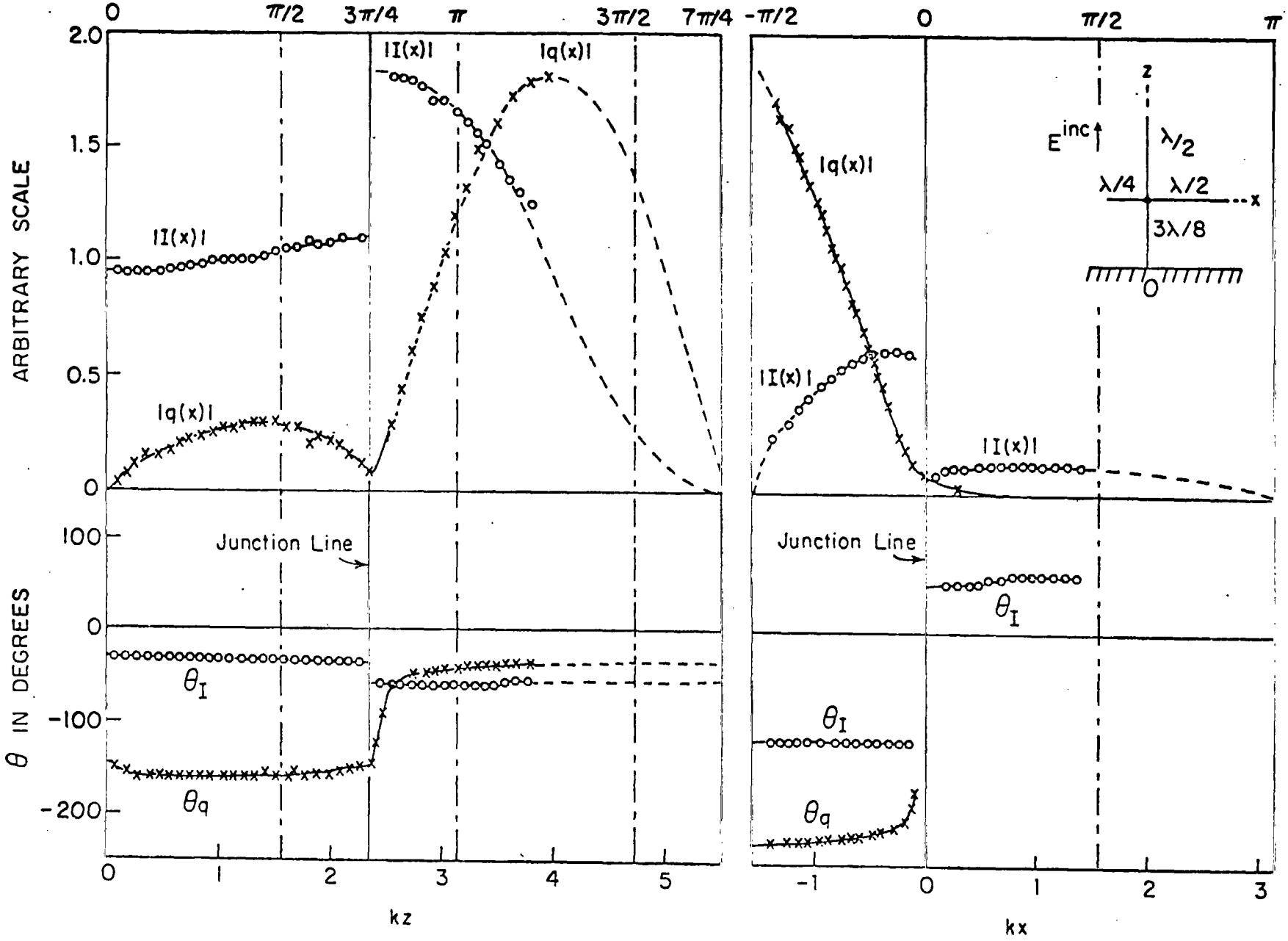

FIG. 10 MEASURED CURRENT AND CHARGE DISTRIBUTIONS ON CROSSED ANTENNA IN NORMALLY INCIDENT FIELD.

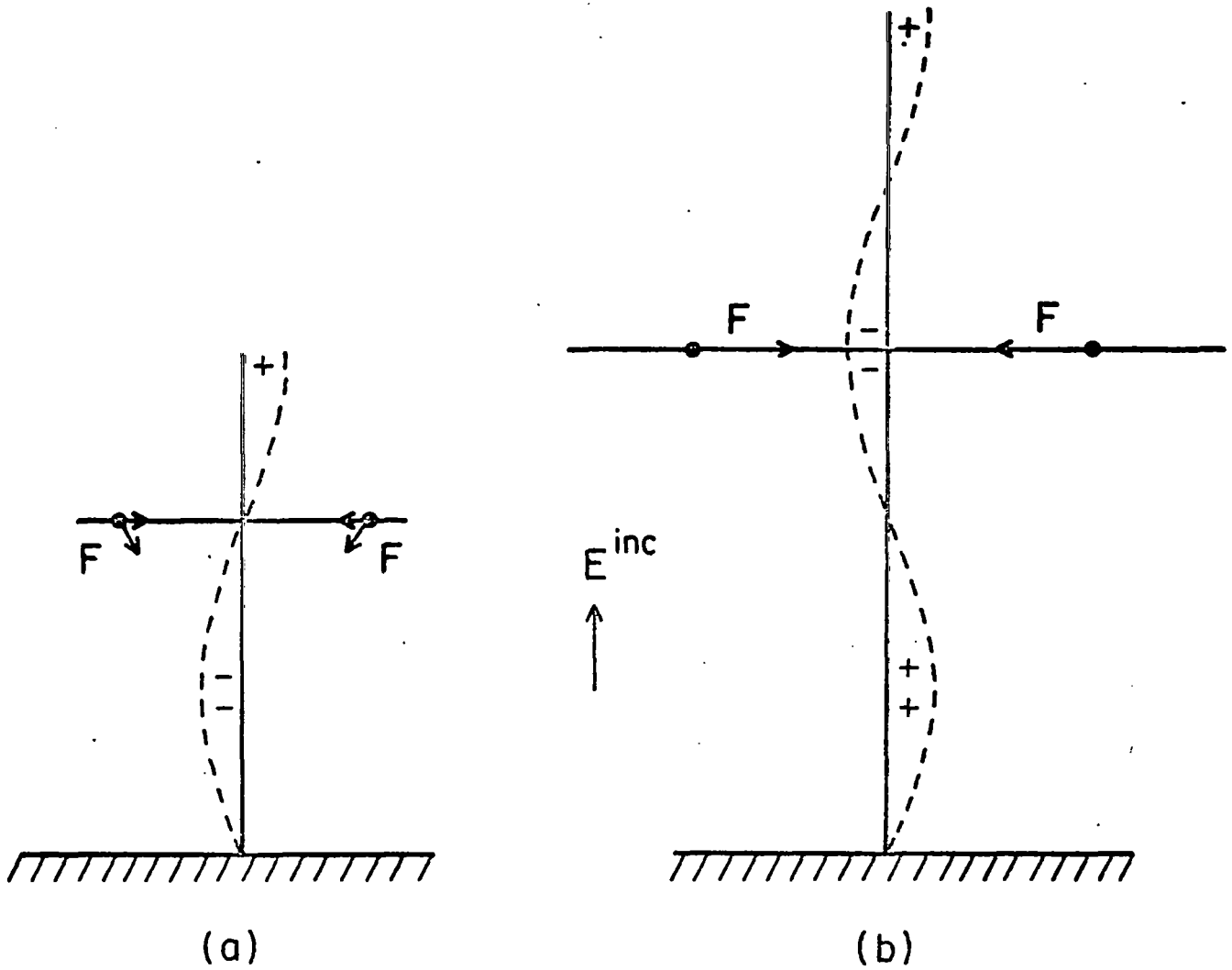

FIG. 11 DIAGRAM TO ILLUSTRATE FORCES ACTING ON CHARGES IN HORIZONTAL WIRE.

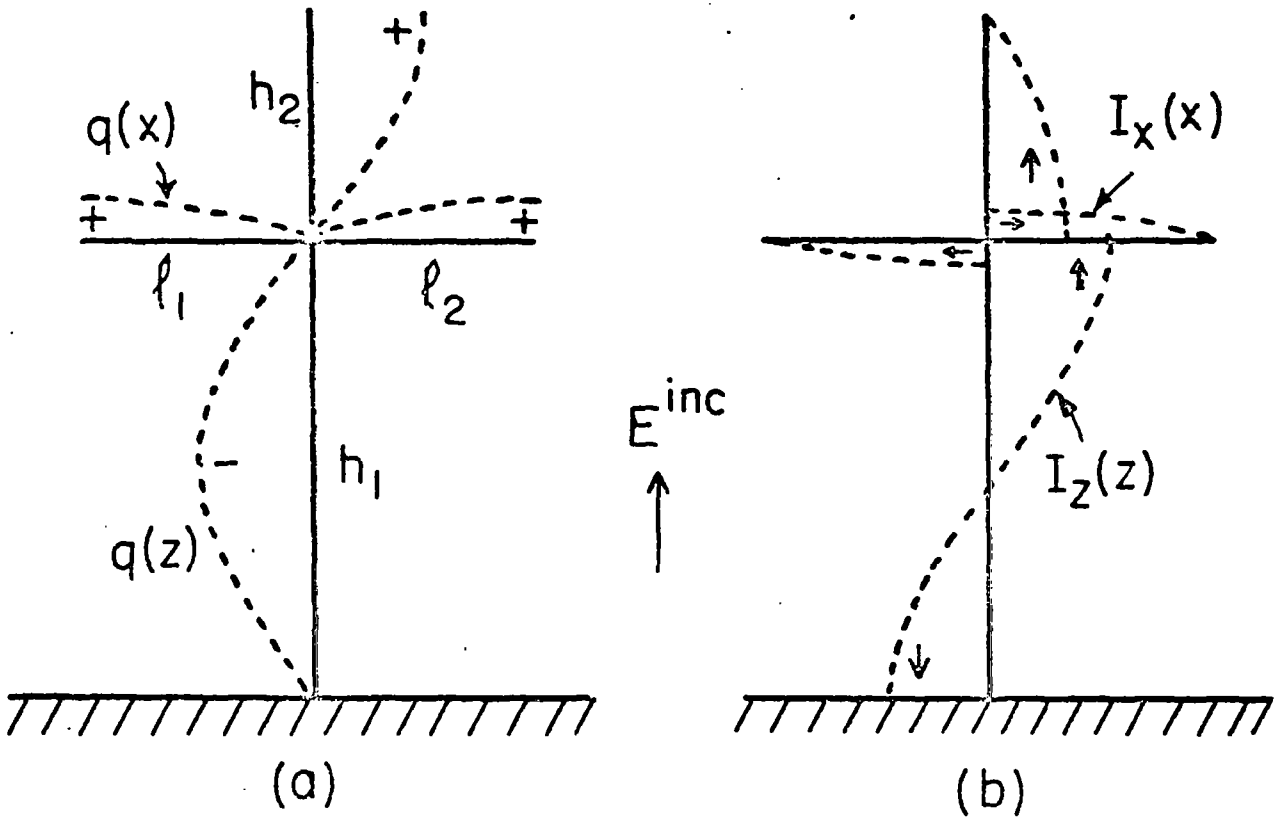

FIG. 12 (a) RESONANT CHARGE PER UNIT LENGTH, (b) RESONANT CURRENT ON CROSSED ANTENNA WITH $kh_1 = \pi$, $kh_2 = k\ell_1 = k\ell_2 = \pi/2$

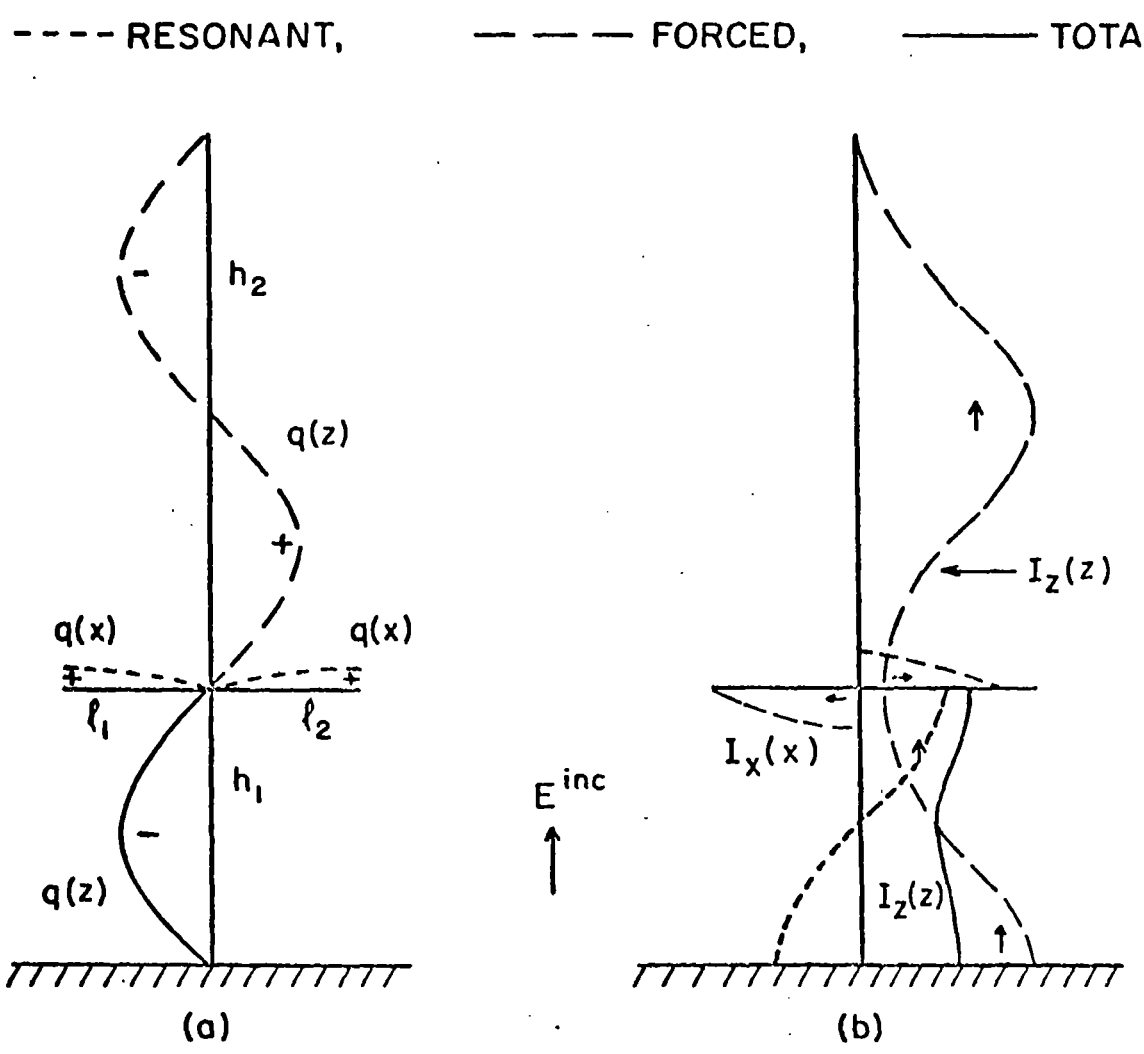

FIG. 13 (a) CHARGE PER UNIT LENGTH, (b) CURRENT ON CROSSED ANTENNA WITH $kh_1 = \pi$, $kh_2 = 2\pi$, $k\ell_1 = k\ell_2 = \pi/2$

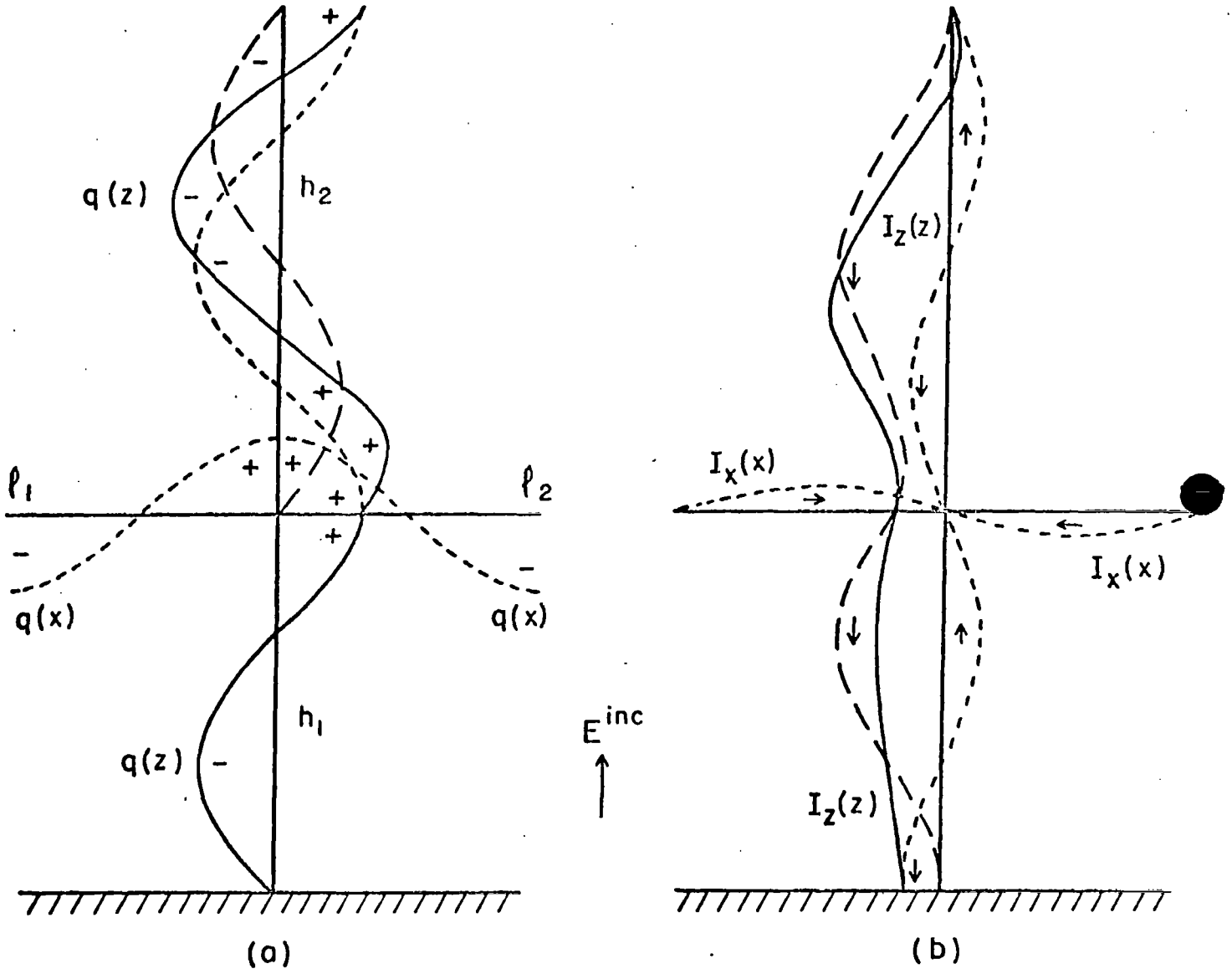

FIG. 14 (a) CHARGE PER UNIT LENGTH; (b) CURRENT ON CROSSED ANTENNA WITH $kh_1 = 3\pi/2$, $kh_2 = 2\pi$, $k\ell_1 = k\ell_2 = \pi$

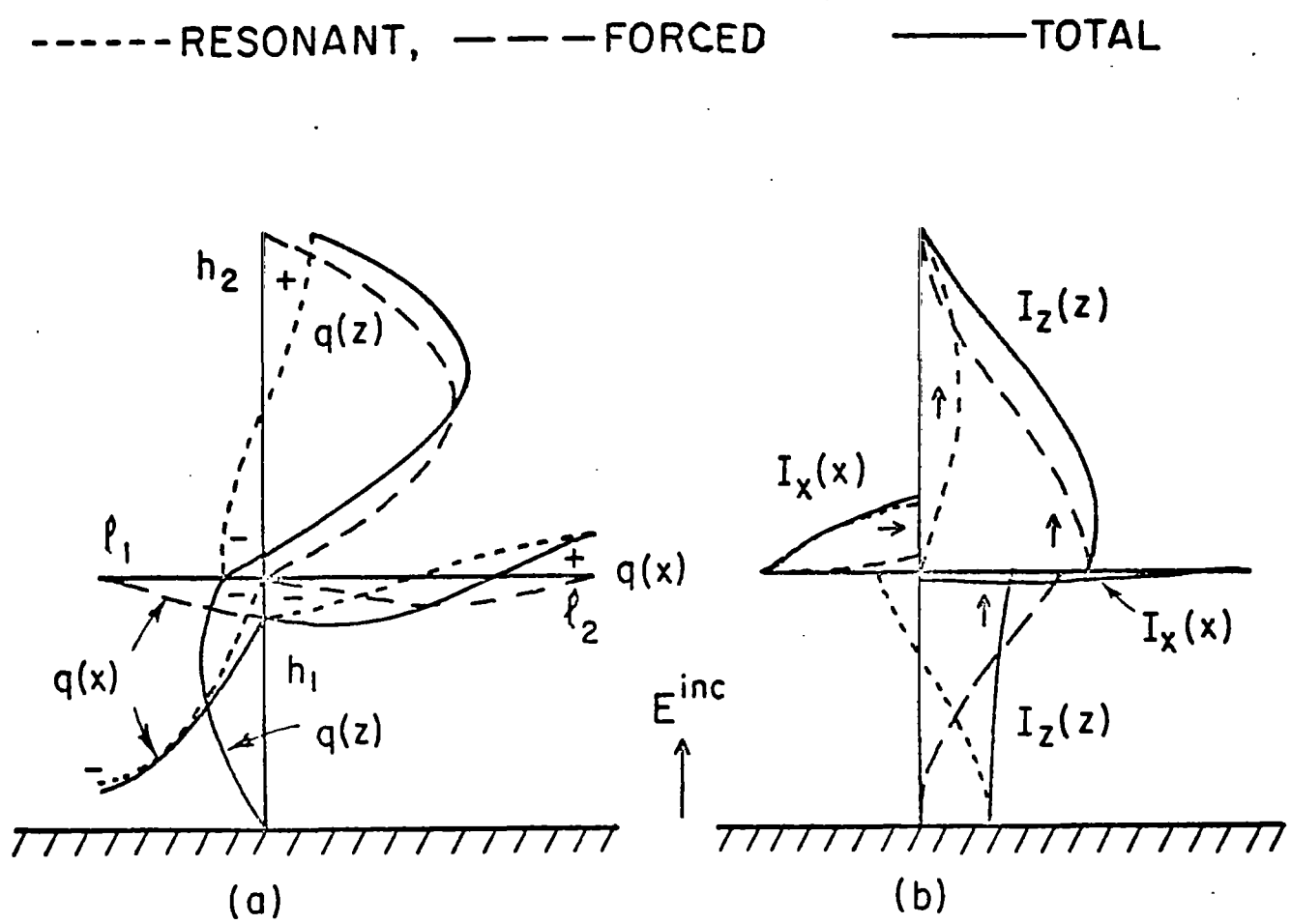

FIG. 15 (a) CHARGE PER UNIT LENGTH, (b) CURRENT ON CROSSED ANTENNAS WITH $kh_1 = 3\pi/4$, $kh_2 = \pi$, $k\ell_1 = \pi/2$, $k\ell_2 = \pi$